CIB-W18/34-12-3

INTERNATIONAL COUNCIL FOR RESEARCH AND INNOVATION IN BUILDING AND CONSTRUCTION

WORKING COMMISSION W18 - TIMBER STRUCTURES

DESIGN MODEL FOR FRP REINFORCED GLULAM BEAMS

by

M Romani

H J Blaß

University of Karlsruhe (TH)

GERMANY

MEETING THIRTY-FOUR

VENICE

ITALY

AUGUST 2001

Design model for FRP reinforced glulam beams

M. Romani and H.J. Blaß
University of Karlsruhe (TH), Germany

1 Abstract

For several years possibilities to reinforce glulam beams parallel to the grain to increase bending and axial stiffness and ultimate load have been investigated. One method is to use Fibre-Reinforced Plastics (FRP) as a tensile reinforcement. Fibres used were glass fibres, aramid fibres and carbon fibres.
At the University of Karlsruhe a research project was carried out where the load-deformation behaviour of reinforced glulam beams was studied. Thin carbon FRP and aramid FRP were used as reinforcements. Within this research project a design model was developed taking into account the plastic behaviour of timber loaded in compression parallel to the grain. This paper presents the design model and test results of beams loaded to failure to verify the design model.

2 Introduction

Glulam beams loaded by bending moments fail at the tension side at the position of knots or finger joints. Due to this failure mode glulam beams are mainly reinforced at the tension side to strengthen the weak cross-sections.
The reinforcement for glulam beams should have a high modulus of elasticity (MOE) and a large tensile strain at failure. Materials considered in the past were steel, glass fibre reinforced plastic (GFRP) and since a few years carbon fibre reinforced plastic (CFRP) and aramid fibre reinforced plastic (AFRP). Fibre reinforced plastic (FRP) has the advantage of a high MOE – although generally lower than steel – and a high tensile strength. The disadvantage of steel is the low yield strength leading to plastic deformations before the timber fails. FRP reinforcements do not show this behaviour.
An effective reinforcement leads to a plastic behaviour on the timber compression side. In unreinforced glulam beams this effect hardly occurs and design models therefore do not take into account this effect. For FRP reinforced beams therefore different design models are necessary.

3 Structure and failure modes of reinforced glulam beams

Figure 1 shows the types of cross section studied. 30 beams of type 1 and 8 beams of type 2 were loaded to failure. In practice, for reasons of fire safety or for esthetical reasons a facing consisting of a load carrying timber lamination is applied below the reinforcement (type 1). Nevertheless 8 beams without a timber facing were tested to study the influence of the timber facing on the load deformation behaviour. The width of the reinforcement always equals the width of the cross section.

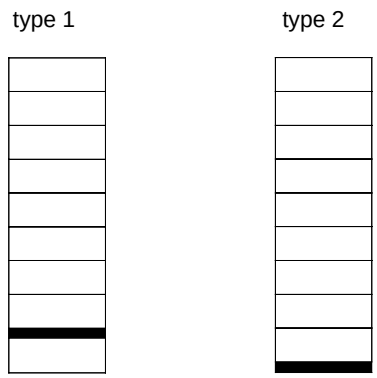

Figure 1: Cross section of the test specimens

For reinforced glulam beams different failure modes are possible. Assuming constant MOE, constant tensile and compressive strength and a linear-elastic-ideal-plastic stress-strain relationship within a cross section the following failure modes are considered.

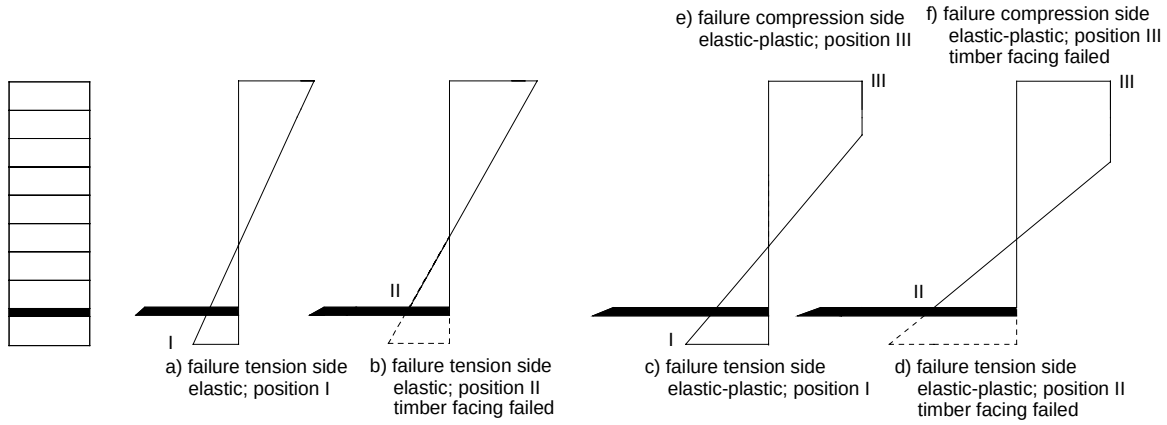

Figure 2: Failure modes

Global failure modes at the tension side:

Mode a: Failure of the timber facing while the cross section is in a linear-elastic state

Mode b: Failure above the reinforcement while the cross section is in a linear-elastic state

Mode c: Failure of the timber facing while the cross section is in a linear-elastic-ideal-plastic state

Mode d: Failure above the reinforcement while the cross section is in a linear-elastic - ideal-plastic state

Failure at the compression side by a defined ultimate compression strain:

Mode e: Compressive failure before the timber facing fails in tension

Mode f: Compressive failure after the timber facing failed in tension with subsequent tensile failure above the reinforcement

Using a tensile reinforcement the compressive stress will exceed the timber tensile stress in beams loaded in bending. Therefore plastic deformations are more probable in beams with tensile reinforcement. Using both, compressive and tensile reinforcement the linear modes will mostly occur due to the reduction of the plastic area in the compressive zone.

4 Design model

Figure 3 illustrates the notation and the assumed stress-strain relation. The design model reduces the calculation to unreinforced glulam beams by using absolute geometrical factors α_i and general factors k_i. These factors allow to calculate geometrically similar cross sections by calculating just once these factors α_i and k_i.

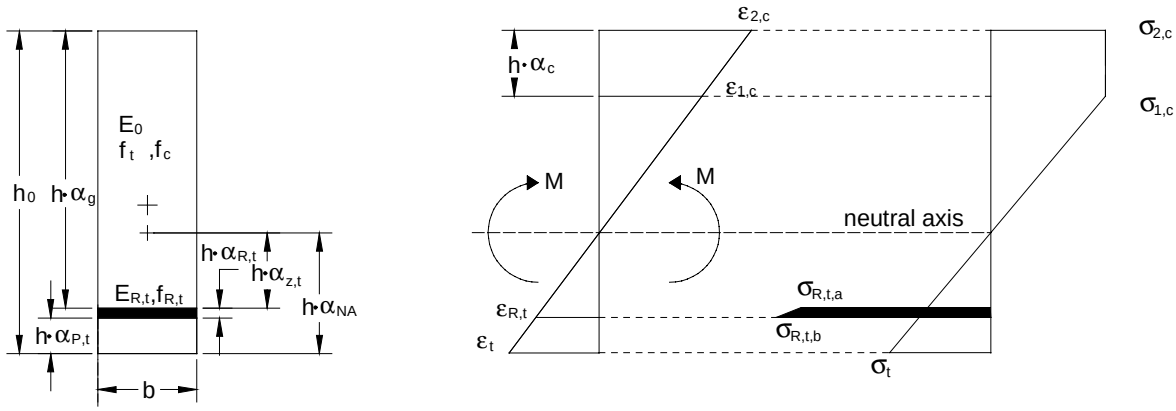

Figure 3: Notation and stress-strain relationship of a type 1 cross section with plastic compression area

Dimensionless factors α_i:

$$\alpha_i = \frac{h_i}{h} \tag{1}$$

Ratio of the timber compressive to tensile strength:

$$k_f = \frac{f_c}{f_t} = \frac{\varepsilon_{c,u}}{\varepsilon_{t,u}} \tag{2}$$

Abbreviation:

$$k_t = \frac{E_{R,t}}{E_0} - 1 \tag{3}$$

The effective height h is the remaining height of the cross section. With intact timber facing h is equal to h_0. After failure of the timber facing the effective height h is reduced by the height of the timber facing.

4.1 Calculation of the load carrying capacity

Because of the non-linear stress distribution, an ultimate moment instead of an ultimate stress is used to express the load carrying capacity. This ultimate moment depends on the failure mode (see figure 2). Failure at the tension side is assumed when the outermost timber fibre of the effective cross section has reached the ultimate strength f_t or the ultimate strain $\varepsilon_{t,u}$, respectively. The strain at the compression side is limited to the ultimate compression strain $\varepsilon_{c,u}$. Below the strain $\varepsilon_{1,c}$ the timber behaves linear-elastic (see Figure 3).

The equilibrium of the resulting forces in the cross-section yields the position of the neutral axis $h \cdot \alpha_{NA}$. After failure of the timber facing the neutral plane changes. The absolute parameters α_i then relate to the reduced height $h = h_0 - h_{P,t}$. Separate equations for cross-sections with or without timber facing are used, because of the different position of the outermost timber fibre below or directly above the reinforcement.

The ultimate moment of a reinforced glulam beam is calculated as:

$$M_u = f_t \cdot W \cdot k_{M,Mode} \tag{4}$$

where: $k_{M,Mode}$ is a failure mode based factor (see figure 2)

$$W = \frac{b \cdot h^2}{6}$$

h: effective height of the beam
f_t: bending strength

The design model is an extension of a design model for tensile bending failure of cross sections without timber facing presented by Ehlbeck and Colling (1987).

4.1.1 Tensile failure

Bending tensile failure is equivalent to reaching the ultimate tensile strain $\varepsilon_{t,u} = \varepsilon_t$ at position I or position II, respectively. According to the observations during the tests failure at position II occurs after failure and subsequent separation of the timber facing (then $h = h_0 - h_{P,t}$) along the beam length.

Mode a ($h = h_0$; $\sigma_{1,t} = f_t$; $\sigma_{1,c} \leq f_c$):

$$\alpha_{NA} = \frac{1}{2} \cdot \frac{1 + \alpha_{R,t} \cdot k_t \cdot (2 \cdot \alpha_{P,t} + \alpha_{R,t})}{1 + \alpha_{R,t} \cdot k_t} \tag{5}$$

$$k_{M,a} = \frac{2}{\alpha_{NA}} \cdot \left[(1 - \alpha_{NA})^3 + \alpha_{NA}^3 - k_t \cdot \left(\alpha_{z,t}^3 - (\alpha_{z,t} + \alpha_{R,t})^3 \right) \right] \tag{6}$$

Mode b ($h = h_0 - h_{P,t}$; $\sigma_t = f_t$; $\sigma_{1,c} \leq f_c$):

$$\alpha_{NA} = \frac{1}{2} \cdot \frac{1 + \alpha_{R,t} \cdot k_t \cdot \alpha_{R,t}}{1 + \alpha_{R,t} \cdot k_t} \tag{7}$$

$$k_{M,b} = \frac{2}{\alpha_{z,t}} \cdot \left[(1 - \alpha_{NA})^3 + (1 + k_t) \cdot \alpha_{NA}^3 - k_t \cdot \alpha_{z,t}^3 \right] \tag{8}$$

Mode c ($h = h_0$; $\sigma_t = f_t$; $\alpha_c \geq 0$):

$$\alpha_{NA} = \frac{1}{(1 + k_f)^2} \cdot \left[k_f - \alpha_{R,t} \cdot k_t + \sqrt{(\alpha_{R,t} \cdot k_t - k_f)^2 + \alpha_{R,t} \cdot k_t \cdot (1 + k_f)^2 \cdot (\alpha_{R,t} + 2 \cdot \alpha_{P,t})} \right. \tag{9}$$

$$\alpha_c = 1 - \alpha_{NA} \cdot (1 + k_f) \tag{10}$$

$$k_{M,c} = 2 \cdot k_f \cdot \left[3 \cdot \alpha_c \cdot \left(1 - \alpha_{NA} - \frac{\alpha_c}{2} \right) + (1 - \alpha_{NA} - \alpha_c)^2 \right] - 2 \cdot \frac{k_t}{\alpha_{NA}} \cdot \left(\alpha_{z,t}^3 - (\alpha_{z,t} + \alpha_{R,t})^3 \right) + 2 \cdot \alpha_{NA}^2 \tag{11}$$

Mode d ($h = h_0 - h_{P,t}$; $\sigma_t = f_t$; $\alpha_c \geq 0$):

$$\begin{aligned} \alpha_{NA} = \frac{1}{(1 + k_f)^2} \cdot \Big[& k_f + \alpha_{R,t} \cdot (k_f \cdot (1 + k_f) - k_t) \\ & + \sqrt{(\alpha_{R,t} \cdot k_t - k_f)^2 + \alpha_{R,t}^2 \cdot k_t \cdot (1 - k_f^{\,2}) - 2 \cdot \alpha_{R,t} \cdot k_f \cdot (1 + k_f)} \Big] \end{aligned} \tag{12}$$

$$\alpha_c = 1 + k_f \cdot \alpha_{R,t} - \alpha_{NA} \cdot (1 + k_f) \tag{13}$$

$$k_{M,d} = 2 \cdot \left[k_f \cdot \left(3 \cdot \alpha_c \cdot \left(1 - \alpha_{NA} - \frac{\alpha_c}{2} \right) + (1 - \alpha_{NA} - \alpha_c)^2 \right) - k_t \cdot \alpha_{z,t}^2 + \frac{\alpha_{NA}^3}{\alpha_{z,t}} \cdot (1 + k_t) \right] \tag{14}$$

Considering a plastic behaviour of a not reinforced cross-section in the compression zone, the factor $k_{M,0}$ according to Ehlbeck and Colling (1987) may be used to calculate the necessary height of a not reinforced beam with the same ultimate moment. The factor $k_{M,0}$ is based on the assumption of a failure at the tension side.

$$h_{M,unrein} = h \cdot \sqrt{\frac{k_{M,Mode}}{k_{M,0}}} \tag{15}$$

where

$$k_{M,0} = \begin{cases} k_f \cdot \dfrac{3 - k_f}{1 + k_f} & k_f \le 1 \\ 1 & k_f > 1 \end{cases} \tag{16}$$

The factor $k_{M,0}$ takes into account that plastic strains are also possible in a not reinforced timber cross section. Inserting $k_{M,0}$ into equation (4) yields the ultimate moment of an unreinforced cross section considering plastic behaviour in the compression zone.
In general, the effect of a plastic compression zone in unreinforced glulam beams is neglected. For a comparison between reinforced and not reinforced glulam beams, however, the same assumptions for the behaviour in the compression zone are made.

4.1.2 Compressive failure

The compressive failure depends on the ultimate strain $\varepsilon_{c,u} = \varepsilon_{2,c}$ at the outermost fibre of the compression zone. A condition for a compressive failure is that no tensile failure occurs, i.e. $\varepsilon_{t,1} \le \varepsilon_{t,u}$.

$$\psi = \frac{\varepsilon_{2,c}}{\varepsilon_{1,c}} \tag{17}$$

Mode e (h= h_0; $\alpha_c \ge 0$, $\varepsilon_{t,u} \ge \varepsilon_t$):

$$\alpha_{NA} = \frac{1}{(\psi - 1)^2} \cdot \left[1 - 2 \cdot \psi - \psi^2 \cdot \alpha_{R,t} \cdot k_t + \psi \cdot \sqrt{2 \cdot \psi + \psi^2 \cdot \alpha_{R,t}^2 \cdot k_t \cdot (k_t + 1)} \right. \\ \left. + 2 \cdot \alpha_{P,t} \cdot (\psi - 1)^2 \cdot \alpha_{R,t} \cdot k_t - 1 + \alpha_{R,t} \cdot k_t \cdot (2 - \alpha_{R,t}) \cdot (2 \cdot \psi - 1) \right] \tag{18}$$

$$\alpha_c = \frac{(1 - \alpha_{NA}) \cdot (\psi - 1)}{\psi} \tag{19}$$

$$k_{M,e} = \frac{2 \cdot k_f}{1 - \alpha_c - \alpha_{NA}} \cdot \left[3 \cdot \alpha_c \cdot \left(1 - \frac{1}{2} \cdot \alpha_c - \alpha_{NA} \right) \cdot (1 - \alpha_c - \alpha_{NA}) + (1 - \alpha_c - \alpha_{NA})^3 \right. \\ \left. + \alpha_{NA}^3 + k_t \cdot (\alpha_{NA} - \alpha_{P,t})^3 - k_t \cdot \alpha_{z,t}^3 \right] \tag{20}$$

$$\varepsilon_{t,u} \ge \varepsilon_{2,c} \cdot \frac{\alpha_{NA}}{1 - \alpha_{NA}} \qquad \text{with } \varepsilon_{t,u} = \frac{f_t}{E_0} \tag{21}$$

Mode f ($h = h_0 - h_{P,t}$; $\alpha_c \geq 0$, $\varepsilon_{t,u} \geq \varepsilon_t$):
By setting $\alpha_{P,t}$ equal to zero and inserting the adjusted α_i in the equations for mode e, the equations for mode f result. This is possible because the modes e and f are independent of the tension stress since no tensile failure occurs. This is checked using equation (22).

$$\varepsilon_{t,u} \geq \varepsilon_{2,c} \cdot \frac{\alpha_{NA} - \alpha_{R,t}}{1 - \alpha_{NA}} \qquad \text{with } \varepsilon_{t,u} = \frac{f_t}{E_0} \tag{22}$$

4.2 Calculation of the bending stiffness

The stiffness is calculated according to the theory of composite cross sections in the linear-elastic state (according to the position of the neutral axis for modes a and b). Plastic deformations are not considered, since the stiffness is used for serviceability limit states.
Stiffness in the linear-elastic state:

$$ef(EI) = \sum n_i \cdot I_i + n_i \cdot A_i \cdot z_i^2 = k_{EI} \cdot E_{0,g} \cdot I \tag{23}$$

$$k_{EI} = \alpha_g^3 + n_t \cdot \alpha_{R,t}^3 + \alpha_{P,t}^3 + 12 \cdot \alpha_g \cdot \left(\frac{1}{2} + \frac{\alpha_{R,t} + \alpha_{P,t}}{2} - \alpha_{NA} \right)^2 + 12 \cdot n_t \cdot \alpha_{R,t} \cdot \left(\alpha_{z,t} + \frac{\alpha_{R,t}}{2} \right)^2 + 12 \cdot \alpha_{P,t} \cdot \left(\alpha_{NA} - \frac{\alpha_{P,t}}{2} \right)^2 \tag{24}$$

with $I = \dfrac{b \cdot h^3}{12}$

α_{NA}: according to mode a or mode b (with $\alpha_{P,t} = 0$)

The factor k_{EI} indicates the stiffness increase of reinforced beams. For not reinforced beams the following height of the cross section is necessary to reach the same bending stiffness:

$$h_{EI,u} = h \cdot \sqrt[3]{k_{EI}} \tag{25}$$

5 Experimental study

30 reinforced glulam beams of type 1 and 8 beams of type 2 were tested to failure. Table 1 summarises the FRP properties, table 2 the adhesives being used and table 3 the test program.

Table 1: FRP

Shortcut.	Type of FRP	Tensile MOE [1)] mean value [N/mm²]	Tensile strength [1)] mean value [N/mm²]	Thickness $h_{R,t}$ [mm]	Width b [mm]
L1	CFRP	173.000	3.050	1,2	100
L2	CFRP	304.000	1.680	1,4	50
L3	AFRP	74.000	995	1,8	132
L4	CFRP	199.000	2.570	1,4	100

[1)] from tension specimen of 50 mm width, average of 5 specimens

Table 2: Adhesives

Shortcut	Name of product	Manufacturer / distribution
K1	Sikadur-30	Sika Chemie GmbH
K2	Ispo Concretin SK 41	ispo GmbH
K3	Collano Purbond HB 110	Ebnöther AG
K4	Dynosol S-199 with H-629	Dyno Industries A.S.

For the test specimens it was decided to use timber with a low MOE and a low density in order to maximise the reinforcement effect. The MOE and the density of every single board was determined before the glulam production. The boards with the smallest MOE and density values were arranged in the outer areas of the cross-section. The mean dynamic MOE of the boards was 9800 N/mm² for MS 10 (according to German Standard DIN 4074) boards which correspond to strength class C24 according to EN 338.
The tests were performed as four point bending tests with a span of 4,20 m and a distance of 1,35 m from the support to the loading point. The thickness of the timber facing was 34 mm (Tr-5;Tr-6) and 35 mm (Tr-1 to Tr-4).

Table 3: Test programme for bending tests

Test series	Number of specimens	Grade of laminations	Grade of timber facing	Mean height/width h_0/b [mm]	FRP (number of layers)	Ad-hesive	Finger joint
Tr-1	5	MS7 / MS10	MS7 / MS10	308/100	L1 (1)	K2	no
Tr-2	5	MS7 / MS10	MS7 / MS10	312/100	L4 (2)	K2	no
Tr-3	5	MS10	MS10	308/100	L1 (1)	K2	yes
Tr-4	5	MS10	MS10	312/100	L4 (2)	K2	yes
Tr-5	5	MS10 / MS17	MS17	312/100	L3 (4)	K3	yes
Tr-6	5	MS10 / MS17	MS10	312/100	L3 (4)	K3	yes
Tr-7	5	MS10	-	308/100	L1 (1)	K3	yes
Tr-8	3	MS10	-	310/100	L4 (2)	K3	yes

The specimens of the test series Tr-1 to Tr-6 first failed due to tensile/bending failure of the timber facing. After the first failure, the load generally could be increased. The timber facing of test specimens with CFRP (FRP L1 and L4) delaminated after failure. The timber facing of test specimens with AFRP (FRP L3) partly failed at two locations and delaminated less than with CFRP. Table 4 shows the test results.

Table 4: Test results

Test series		Tr-1	Tr-2	Tr-3	Tr-4	Tr-5	Tr-6	Tr-7	Tr-8
F_{max}	[kN]	44,1	57,7	43,0	58,1	60,5	59,1	49,8	66,5
$M_{u,mean}$	[kNm]	59,5	77,9	58,1	78,4	81,7	79,8	67,2	89,8
$f_m = M_{u,mean}/W$	[N/mm²]	37,6	48,0	36,7	48,3	50,4	49,2	42,5	56,1
COV	[%]	12,5	4,7	13,0	5,9	6,8	3,5	5,0	6,9
Deflection	[mm]	70,2	86,6	64,0	97,5	88,6	83,2	61,7	74,8
COV	[%]	16,1	6,5	33,4	5,8	12,1	6,6	4,8	12,3
Failure at (number)		K (5)	K (5)	K (3) F (2)	K (1) F (3) T (1)	F (3) A (2)	K (1) F (2) A (2)	K (2) F (3)	K (2) F (1)
Failure mode (number)		c (1) d (4)	d (4) f (1)	c (3) d (2)	d (5)	c (3) d (2)	d (4) f (1)	d (5)	d (3)
ef MOE	[N/mm²]	10.400	11.400	10.300	11.500	12.700	12.200	11.100	13.100
COV	[%]	5,9	4,2	1,7	5,0	4,5	2,3	3,6	0,9

K: knot T: timber
F: finger joint A: abort of test

In Figure 4 the load-deflection curve of test specimen Tr-3.4 is presented with a first failure at the timber facing, a consequent global failure starting above the reinforcement after 30 % load increase.

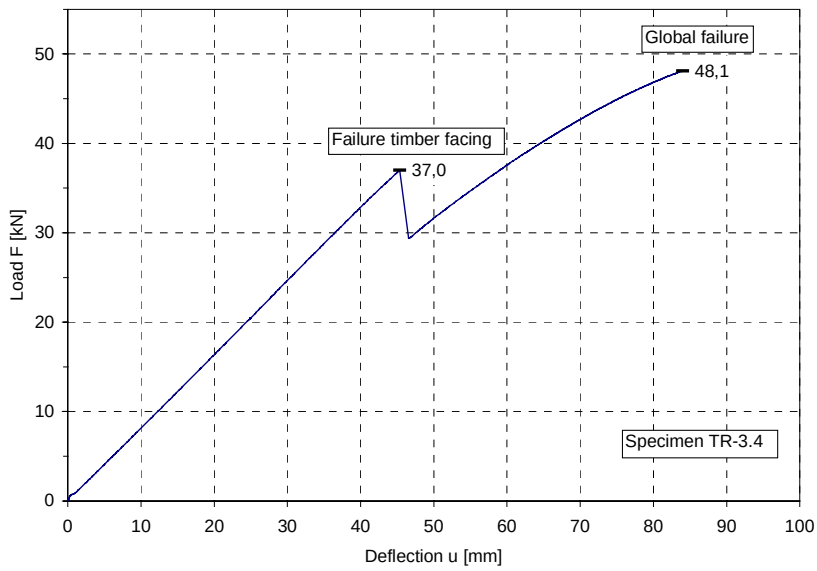

Figure 4: Load deflection curve of test specimen Tr-3.4

6 Comparison of the Design model with the test results

The calculation model allows to design reinforced beams according to Eurocode 5. As input values for the glulam strength and MOE the values according to glulam BS 11 of the German National Application Document for Eurocode 5 are applied. This strength class is very similar to GL 24. For the modes e and f $\varepsilon_{2,c}$ was set to 1,3 times $\varepsilon_{1,c}$.

Table 5: Material properties for the calculation model

	f_t [N/mm²]	f_c [N/mm²]	k_f [-]	MOE [N/mm²]
Glulam BS11/GL24	24,0 (=$f_{m,g,k}$)	24,0 (=$f_{c,0,g,k}$)	1,00	11.500
CFRP L1	3.050	-	-	173.000
AFRP L3	995	-	-	74.000
CFRP L4	2.570	-	-	199.000

Because of $f_t = f_c$ only modes c, d, e and f are possible.

Table 6: Ultimate Moment capacity according to the calculation model

Mode			Tr-1	Tr-2	Tr-3	Tr-4	Tr-5[1)]	Tr-6[1)]	Tr-7	Tr-8
c	$M_{u,c}$	[kNm]	43,0	51,9	43,0	51,9	49,9	49,9	NP	NP
	α_c	[-]	0,042	0,109	0,040	0,108	0,091	0,091		
	$M_{u,mean}/M_{u,c}$	[-]	1,38	1,50	1,35	1,51	1,64	1,60		
d	$M_{u,d}$	[kNm]	37,4	50,1	37,2	49,8	48,4	48,4	46,3	60,1
	α_c	[-]	0,066	0,176	0,064	0,177	0,173	0,173	0,059	0,158
	$M_{u,mean}/M_{u,d}$	[-]	1,59	1,55	1,56	1,57	1,69	1,65	1,45	1,49
e	$M_{u,e}$	[kNm]	49,2	53,6	53,0	53,5	52,6	52,6	NP	NP
	α_c	[-]	0,122	0,128	0,121	0,128	0,127	0,127		
	$\sigma_{t,required}$	[N/mm²]	28,0	24,9	28,1	24,9	25,6	25,6		
f	$M_{u,f}$	[kNm]	51,9	59,6	55,8	59,6	57,9	57,9	51,4	58,9
	α_c	[-]	0,124	0,133	0,123	0,133	0,131	0,131	0,123	0,133
	$\sigma_{t,required}$	[N/mm²]	27,0	22,8	27,1	22,8	23,7	23,7	27,3	22,8

NP: Mode not possible

[1)] The MS 17 timber lamella was not considered.

The design model relates to a beam cross-section. Because of the not complete delamination of the timber facing for different adhesive-FRP combinations, the assumption of a complete delamination over the length of the beam is conservative.

The comparison shows a mean ratio of about 1,49 between the load-carrying capacity in the test and the governing calculated characteristic load-carrying capacity. The characteristic value of that ratio based on the single test results is 1,24, the minimum value from 38 tests is 1,18. Taking into account the unfavourable lamination properties, the calculation model yields conservative values of the beam bending capacity.

In Table 7 a fictitious MOE as a parameter for the bending stiffness of the test series and the calculated MOE values are summarised. For every board used in the glulam beams the dynamic, lengthwise MOE was measured before glulam production. The calculated MOE of the beams were determined using the MOE of every single board with the theory of composite

cross section for the elastic state. In row 1 the measured values of the test specimens, in rows 2 and 3 the calculated values of the reinforced and unreinforced beams are presented.

Table 7: Calculated MOE versus MOE of the test series

			Tr-1	Tr-2	Tr-3	Tr-4	Tr-5	Tr-6	Tr-7	Tr-8
1	$MOE_{rein.,test}$	[N/mm²]	10.400	11.400	10.300	11.500	12.700	12.200	11.100	13.100
2	$MOE_{rein.,calc}$	[N/mm²]	10.100	11.100	10.300	12.000	13.500	12.900	11.100	13.700
3	$MOE_{unrein.,calc}$	[N/mm²]	9.100	8.700	9.200	9.300	11.500	10.800	9.400	9.300
4	1 / 2	[-]	1,03	1,03	1,00	0,96	0,94	0,95	1,00	0,96
5	1 / 3	[-]	1,14	1,31	1,12	1,24	1,10	1,13	1,18	1,41

The calculated values of the fictitious MOE with the composite theory assuming a stiff connection between the reinforcement and the glulam show a good agreement with the test results.

7 Summary

For the calculation of the load-carrying capacity and stiffness of tensile reinforced glulam beams a model is derived taking into account the plastic behaviour of glulam loaded in compression parallel to the grain. The model is based on an analytic solution and allows a simple calculation without any iteration steps based on design values of non-reinforced glulam. Different failure modes of FRP reinforced glulam beams are considered. Test results with reinforced beams loaded to failure show that the proposed model leads to conservative values of the load-carrying capacity. This is especially true considering the low quality of the timber used in the tests.

The test specimens mainly failed at the tension side. With a different cross-section set-up reinforced beams are possible failing in a more ductile way on the compression side. The test specimens mostly showed a significant load increase after failure of the timber facing. This was mainly caused by an effective reinforcement even after a bending failure above the FRP layer. Further research will quantify this effect and permit a more economic use of FRP reinforced glulam.

References

Blaß HJ and Romani M (2000) Trag- und Verformungsverhalten von Verbundträgern aus Brettschichtholz und faserverstärkten Kunststoffen. Forschungsbericht der Versuchsanstalt für Stahl, Holz und Steine, Abt. Ingenieurholzbau der Universität Karlsruhe

Ehlbeck J and Colling F (1987) Tragfähigkeit von Glasfaser-Verbund-Profilen verstärkten Brettschichtholzträgern. Forschungsbericht der Versuchsanstalt für Stahl, Holz und Steine, Abt. Ingenieurholzbau der Universität Karlsruhe